



Adsorption Behaviour, Thermodynamic and Electrochemical Studies of Chloro Derivatives of N-(4-methoxybenzylidene)aniline as corrosion inhibitors for zinc in hydrochloric acid

S. Kumar, D. Ladha and N.K. Shah*

Department of Chemistry, School of Sciences, Gujarat University, Ahmedabad- 380009, Gujarat, India.

Received 22 Sept 2013, Revised 25 Feb 2014, Accepted 25 Feb 2014

*Corresponding author. E-mail: nishchem2004@yahoo.co.in; Tel No. (+9107926305037)

Abstract

The inhibitive action of chloro derivatives of N-(4-methoxybenzylidene)aniline on the corrosion of zinc in hydrochloric acid solution has been investigated by weight loss, galvanostatic polarization and electrochemical impedance spectroscopy (EIS) techniques. Corrosion inhibition efficiency increases with increase in inhibitors concentration and is maximum at $20.4 \times 10^{-3} \text{ mol L}^{-1}$. Thermodynamic parameters such as Q_{ads} , $\Delta G_{\text{ads}}^{\circ}$ and activation energies (E_a) were calculated. $\Delta G_{\text{ads}}^{\circ}$ values show that studied inhibitors exhibit complex type of interaction with metal surface i.e. both physical as well as chemical adsorption. The polarization measurements indicated, mixed type of inhibition at lower concentration and cathodic at higher concentration. The adsorption of inhibitors on zinc obeyed Langmuir's isotherm.

Keywords: Zinc, Weight loss, Polarization, EIS, Acid inhibition.

1. Introduction

For scale removal and cleaning of zinc surface with acid solutions, the use of organic inhibitors is one of the most practical methods for protection against corrosion [1-14]. Corrosion inhibition efficiency of organic compounds is connected with their adsorbing power. The role of the adsorbed inhibitor is to isolate the corroding metal from corrosive medium and/or to modify the electrode reactions which cause dissolution of the metal. Zinc is an active metal which dissolves readily in acid media. Therefore, there is a strong necessity for the protection of zinc by organic inhibitors. Those compounds, which have hetero atoms (N, O, P and S) in their aromatic ring, are most successful inhibitors. Some research work [5, 16-18] reveals that the inhibition efficiency of Schiff bases is much greater than that of corresponding amines and aldehydes. This may be due the presence of a $>C=N-$ group in these molecules. The aim of this work is to study the corrosion inhibition of zinc in HCl solution using gravimetric measurements, electrochemical techniques such as galvanostatic polarization and electrochemical impedance spectroscopy measurements. The inhibitors investigated are: 2-Chloro-N-(4-methoxybenzylidene)aniline (2-CNMBA), 3-chloro-N-(4-methoxybenzylidene)aniline (3-CNMBA), and 4-chloro-N-(4-methoxybenzylidene)aniline (4-CNMBA).

2. Material and Methods

2.1 Preparation of Schiff bases

The Schiff bases were synthesized by condensation of 4-methoxybenzaldehyde with 2-chloroaniline, 3-chloroaniline and 4-chloroaniline in the presence of ethyl alcohol as per the procedure described by Shah et al [19]. 2-CNMBA (boiling point: 362.4°C . registry no. is not available) is dark reddish liquid, 3-CNMBA (boiling point: 335.9°C , Registry number: 24776-57-6) is brownish liquid and 4-CNMBA (melting point: 335.9°C , Registry number: 15485-22-0) is a white crystalline solid. These compounds are insoluble in water but soluble in ethanol, methanol, ethyl acetate and THF. These compounds have been previously tested as inhibitors for Al-Mg alloy in HCl [20]. The compounds were characterised through IR spectroscopy. The molecular structures of the Schiff bases are shown in Figure 1(a, b and c).

2.2 Preparation of Specimens

Rectangular specimens of electrolytic zinc, of size 3.0 cm × 3.0 cm (thickness = 0.139 cm) with a small hole of about 2 mm diameter just near one end of the specimen were used for the determination of the corrosion rate. The specimens were grinded using successively '0' to '0000' Oakey emery paper. The polishing was done using jewellers rouge, which gave mirror-like finish. The specimens were washed with ethanol and finally with distilled water and then dried at room temperature. The dried and weighed specimens were exposed to 230 mL of 0.5 M and 1.0 M HCl solution containing controlled additions of various Schiff bases in the range of 6.11×10^{-3} to 20.37×10^{-3} (molL⁻¹). One specimen was suspended by a pyrex glass hook in each beaker of the test solution, which was open to the air at 35 ± 0.5 °C, to the same depth of about 1.5 cm below the surface of the liquid.

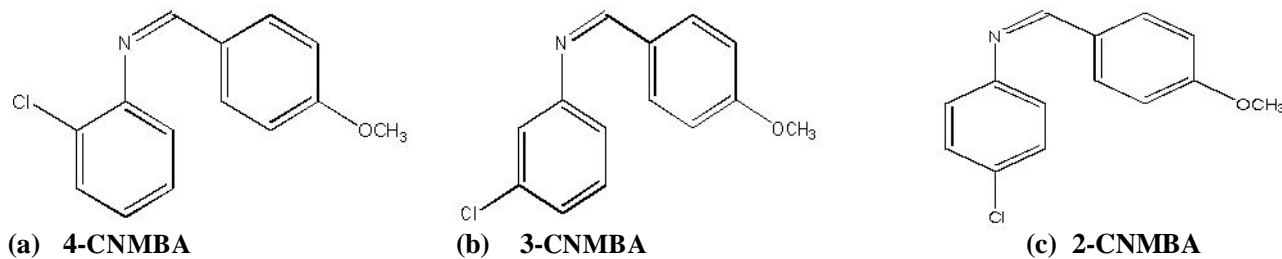


Figure 1: Molecular Structure of studied compounds (a) 4-CNMB (b) 3-CNMB (c) 2-CNMB.

The weight of the specimen before and after immersion was determined using mettler balance - M5 type. The triplicate experiments were performed. The effect of temperature ($35 - 65$ °C) on the corrosion of zinc in 0.5 M and 1.0 M HCl in the presence of 6.11×10^{-3} and 20.37×10^{-3} (molL⁻¹) concentrations of inhibitors was studied using weight loss measurements. Effect of exposure period on inhibition efficiency was also carried out at 6.11×10^{-3} and 20.37×10^{-3} (molL⁻¹) concentration of inhibitors at temperature $35^\circ\text{C} \pm 0.5$ °C. Corrosion rate and percentage inhibition efficiency (% IE) were calculated.

2.3 Galvanostatic polarisation studies

For polarisation studies, metal coupons of circular design, diameter 2.802 cm with a handle 3.0 cm long and 0.139 cm wide were used. The handle and the back of the coupon and of the auxiliary platinum electrode were coated with perspex leaving only circular portion of the specimen exposed (apparent surface area, 6.156 cm²) to the solution. The solution 80 ml in each limb was contained in an H – type pyrex glass cell with the Luggin capillary as near to the electrode surface as possible and a porous partition was used to separate the two electrodes.

Polarisation was carried out using a three-electrode cell assembly where zinc was used as working electrode, platinum as counter electrode and saturated calomel electrode (SCE) as reference electrode. In these experiments, the current density was varied in the range 1.62×10^{-4} to 32.5×10^{-3} Acm⁻². The corrosion parameters such as corrosion potential (E_{corr}), corrosion current density (I_{corr}) and Tafel plots were measured in polarisation method.

2.4 Electrochemical impedance spectroscopy (EIS) studies

EIS studies were performed in 30 kHz to 1 Hz frequency range using Autolab PGSTAT 302N. EIS data were obtained at the corrosion potential (E_{corr}) of the working electrode (metal coupons of circular design, diameter 2.802 cm with a handle 3.0 cm long and 0.139 cm wide were used) measured against Ag/AgCl reference electrode using a 5 mV rms sinusoidal perturbation. The impedance parameters were calculated by fitting the experimental results to an equivalent circuit using NOVA 1.9.16 software.

3. Results and Discussion

3.1 Weight loss method

The inhibition efficiency (?) and the degree of surface coverage (?) were calculated using following equations:

$$\text{Inhibitor efficiency (?)} = \frac{W_u - W_i}{W_u} \times 100\% \quad (1)$$

$$\text{Surface coverage (?)} = \frac{W_u - W_i}{W_u} \quad (2)$$

where, W_u = weight loss of zinc in uninhibited acid and W_i = weight loss of zinc in inhibited acid

It is clear from Table 1 that weight loss of zinc decreases sharply and the inhibition efficiency increases when the concentration of inhibitors increases. Maximum inhibition efficiency is attained in the presence of $20.37 \times 10^{-3} \text{ molL}^{-1}$ of all the inhibitors. Therefore, we can say that the inhibition found to depend on inhibitor's concentration. The inhibitory action of inhibitors against zinc corrosion attributed to the adsorption of its molecules on the zinc surface, which limits the dissolution of the latter by blocking its corrosion sites and decreasing the weight loss thereby increasing inhibition efficiency as the concentration increases. These results indicate that all the Schiff bases are excellent corrosion inhibitors for zinc in hydrochloric acid.

Table 1: Corrosion parameters for Zinc in aqueous solution of 0.5 M and 1.0 M HCl in absence and presence of different concentrations of inhibitors from weight loss measurements at $35 \pm 0.5^\circ\text{C}$ for 30 min.

Inhibitors and Its concentration	Concentration of HCl			
	0.5 M HCl		1.0 M HCl	
molL^{-1}	Weight Loss mg/dm^3	%Inhibition efficiency	Weight Loss mg/dm^3	%Inhibition efficiency
HCl only	7930		16246	
4-CNMBA				
6.11×10^{-3}	1041	86.87	13157	19.01
8.15×10^{-3}	66	99.17	13056	19.64
12.22×10^{-3}	23	99.71	4582	71.80
16.29×10^{-3}	20	99.74	264	98.37
20.37×10^{-3}	1	99.98	15	99.91
3-CNMBA				
6.11×10^{-3}	1168	85.27	15748	3.07
8.15×10^{-3}	76	99.04	13650	15.98
12.22×10^{-3}	25	99.68	4978	69.36
16.29×10^{-3}	20	99.74	401	97.53
20.37×10^{-3}	6	99.92	17	99.90
2-CNMBA				
6.11×10^{-3}	4267	46.19	15850	2.44
8.15×10^{-3}	2682	66.18	14326	11.82
12.22×10^{-3}	589	92.57	6843	57.88
16.29×10^{-3}	229	97.12	1367	91.59
20.37×10^{-3}	71	99.10	298	98.16

3.2 Adsorption isotherm and thermodynamic parameters

The adsorption of the inhibitor at the metal-solution interface is the first step in the inhibition mechanism in aggressive media. There are three possibilities of adsorption which may take place by organic molecules at the metal - solution interface: (i) electrostatic attraction between the charged metal and the charged molecules, (ii) interaction of p electrons with the metal and (iii) combination of (i) and (ii) [5]. The adsorption isotherms are useful for acknowledging the mechanism of corrosion inhibition.

The values of surface coverage (θ) for the different concentrations of the studied inhibitors at $35^\circ\text{C} \pm 0.5^\circ\text{C}$ were used to explain the best adsorption isotherm to determine the adsorption process. Attempts were made to fit θ values to various isotherms including Langmuir, Temkin and Freundlich isotherms. Among the three isotherms obtained, the best fitted was Langmuir adsorption isotherm. Plotting of C_{inh} / θ against C_{inh} gave a straight line as shown in Figure 2 (a, b and c) indicating the adsorption of Schiff base compounds namely 4-CNMBA, 3-CNMBA and 2-CNMBA on the zinc surface follow the Langmuir adsorption isotherm as it can be seen that the slopes and R^2 values for the Langmuir plots of these inhibitors are very close to unity [21, 22, 23] which can be expressed as according to Equation (3).

$$\frac{C_{inh}}{\theta} = \frac{1}{K_{ads}} + C_{inh} \quad (3)$$

where, K_{ads} is the equilibrium constant of the adsorption process, C_{inh} is the concentration of inhibitor.

The relation between equilibrium constant of adsorption, K_{ads} and standard free energy change of adsorption (ϵG_{ads}^o) is given by:

$$\epsilon G_{ads}^o = - 2.303RT \log (55.5 K_{ads}) \quad (4)$$

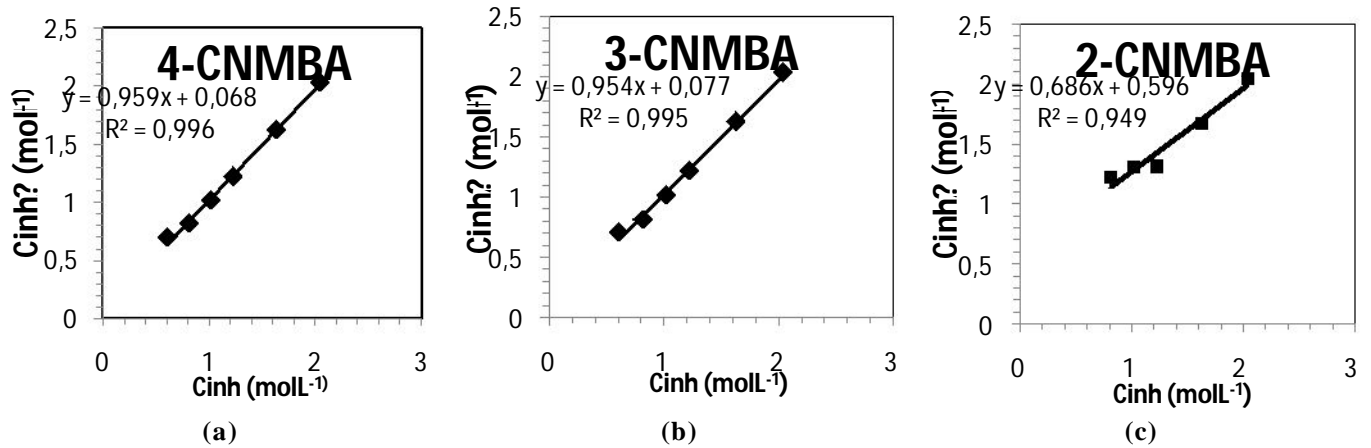


Figure 2: Langmuir plots for studied Schiff bases in 0.5M HCl at 35± 0.5°C (a) 4-CNMBA (b) 3-CNMBA (c) 2-CNMBA

Table 2: Standard free energy of adsorption (ϵG_{ads}^o) of Schiff bases during the corrosion of zinc in 0.5 M HCl

Inhibitor	Inhibitor molL ⁻¹	Thermodynamic parameters	
		ϵG_{ads}^o (kJ/mol)	k_s (kJ/mol)
4-CNMBA	6.11 * 10 ⁻³	-27.45	-70.63
	20.37 * 10 ⁻³	-36.36	-53.97
3-CNMBA	6.11 * 10 ⁻³	-26.69	-67.91
	20.37 * 10 ⁻³	-34.43	-88.03
2-CNMBA	6.11 * 10 ⁻³	-22.09	-48.45
	20.37 * 10 ⁻³	-30.17	-54.39

The values of the standard free energy of adsorption (ϵG_{ads}^o) calculated from the Equation (4) are given in table 2. The large negative values of ϵG_{ads}^o ensure the spontaneity of the adsorption process and the stability of the adsorbed layer on the zinc surface [24-28]. Generally, ϵG_{ads}^o values between 0 and -20kJ mol⁻¹ are associated with electrostatic interactions between the charged molecules and the charged metal surface (physisorption), whereas those below - 40 kJmol⁻¹ involve the sharing or transfer of charge from the organic molecules to the metal surface to form a coordinate covalent bond (chemisorption) [29-31]. The values of ϵG_{ads}^o are negative which indicate that the adsorption of inhibitor molecules on the metal surface is a spontaneous process. The negative values of ϵG_{ads}^o obtained for inhibitors 2-CNMBA, 3-CNMBA and 4-CNMBA are more than 20 kJmol⁻¹ and less than 40 kJmol⁻¹ indicating that the adsorption process of the evaluated inhibitors on the zinc surface may involve complex type of interactions i.e. both chemisorption and physisorption mechanism. The studied inhibitors obey the general rule that the effectiveness of corrosion inhibition increases with increasing the negative values of ϵG_{ads}^o (kJmol⁻¹) and follow the trend: 4-CNMBA > 3-CNMBA > 2-CNMBA. The trend is in accordance with the inhibition efficiencies.

An estimate of heat of adsorption, (Q_{ads}), of the inhibitors can be calculated from the trend of surface coverage (θ) with temperature as follow Equation (5) [32].

$$Q_{ads} = 2.303R \left[\log \frac{\epsilon_2}{1 - \epsilon_2} - \log \frac{\epsilon_1}{1 - \epsilon_1} \right] \frac{T_1 T_2}{T_2 - T_1} \quad (5)$$

where, ϵ_1 and ϵ_2 are the fractions of the total surface, covered by the inhibitors at temperatures T_1 (K) and T_2 (K) respectively. The negative values of Q_{ads} (Table 2) (ranges from - 48.45 kJmol⁻¹ to - 88.03 kJmol⁻¹) in all cases show that the adsorption of inhibitors on zinc surface is exothermic and hence inhibition efficiency decreases with rise in temperature. Since the reactions are carried out at constant pressure, calculated values of Q_{ads} are expected to be approximately equal to the enthalpy change [28].

3.3 Effect of temperature

To study the effect of temperature on the inhibition efficiency of the three inhibitors, weight losses were determined in 0.5 M HCl containing 6.11×10^{-3} molL⁻¹ and 20.37×10^{-3} of 2-CNMBA, 3- CNMBA and 4- CNMBA at solution temperatures of 35, 45, 55 and 65 °C (Table 3).

Logarithmic form of Arrhenius equation (6) was used to calculate the apparent activation energy for the corrosion of zinc in the absence and presence of inhibitors.

$$\log i = \log A - \frac{E_a}{2.303RT} \quad (6)$$

where, i is the corrosion rate, E_a is the apparent activation energy, T is the temperature and A is constant.

Plotting $\log i$ versus $(1/T) \times 10^3$ gave a straight line with slope of $-\frac{E_a}{2.303RT}$ in Figure 3 (a and b).

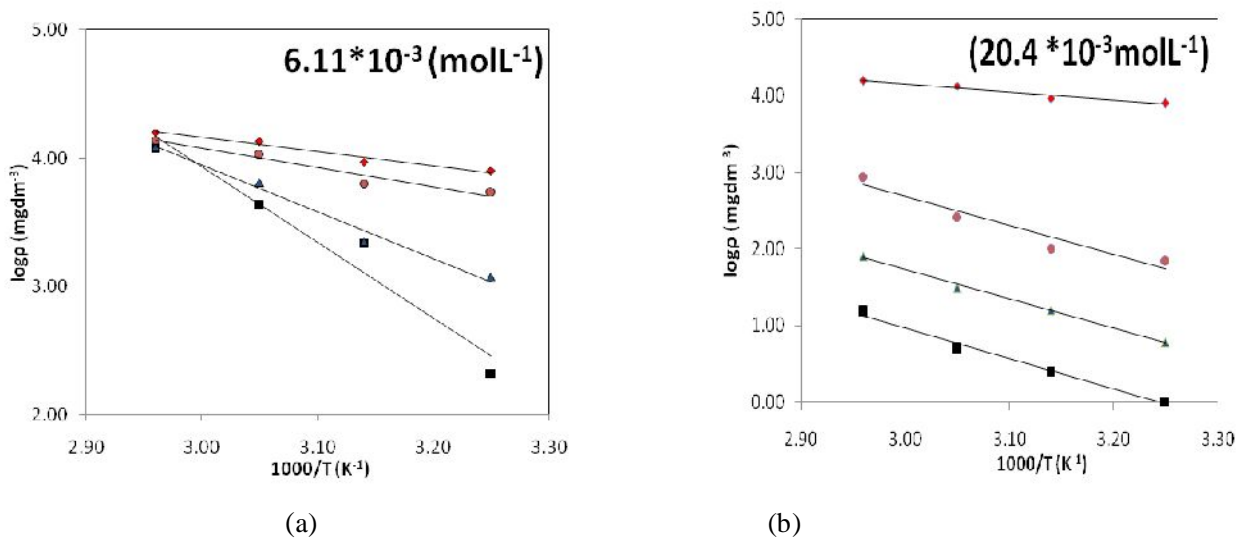


Figure 3: Arrhenius plots for Zinc in 0.5M HCl in the presence and absence of (a) 6.11×10^{-3} and (b) 20.37×10^{-3} (molL⁻¹inhibitor concentration [Blank (□...□); 2-CNMBA (○...○); 3-CNMBA (△...△); 4-CNMBA (◇...◇)])

The results given in Table 3 show that in plain as well as in acid containing inhibitors, the corrosion rate increases and as a result, the inhibition efficiency decreases with rise in temperature. This may be due to desorption of the inhibitor molecules at higher temperatures, thus exposing the metal to further attack.

The apparent activation energies calculated from Equation (6) are presented in Table 3. From the results obtained, it can be seen that the activation energies in the presence of inhibitors (ranging from 35 to 112.9 kJmol⁻¹) are greater than in the absence of inhibitors (E_a for the blank = 21.38 kJmol⁻¹) indicating that the corrosion of zinc is retarded by the presence of inhibitors [33]. The results also indicate that the apparent activation energy increases with increasing concentration of inhibitors which further suggests that there is increasing tendency of adsorption of the inhibitors with increase in concentration [34-36].

3.4 Galvanostatic polarization measurements

The anodic dissolution of zinc and the cathodic evolution of hydrogen were carried out by galvanostatic polarisation in HCl solution, plain as well as with inhibitor. The galvanostatic polarization curves of zinc in 0.5 M

HCl and in the presence of two concentrations (6.11×10^{-3} and 20.37×10^{-3} (molL⁻¹) of 4-CNMBA, 3- CNMBA and 2- CNMBA shown in Figure 4 (a and b). It is observed that in the presence of inhibitors, both the cathodic and anodic curves show lower current density than those observed in the uninhibited solution.

Table 3: Effect of temperature on weight loss and inhibition efficiency (percentage) and E_a of Schiff bases for zinc in 0.5 M HCl.

Inhibitor	Inhibitor Concentration molL ⁻¹	Weight loss, mg/dm ² , at a temperature of				Energy of Activation(E_a) (kJmol ⁻¹)
		35± 0.5 °C	45± 0.5 °C	55± 0.5 °C	65± 0.5 °C	
HCl only	-----	7930	9439	13553	16017	21.38
4-CNMBA	6.11×10^{-3}	1041 (86.87%)	2169 (77.02%)	4384 (67.65%)	12156 (24.10%)	76.19
	20.37×10^{-3}	1 (99.98%)	3 (99.97%)	5 (99.96%)	15 (99.91%)	112.93
3-CNMBA	6.11×10^{-3}	1168 (85.27%)	2235 (76.32%)	6406 (52.73%)	10714 (20.95%)	70.40
	20.37×10^{-3}	7 (99.91%)	16 (99.83%)	31 (99.77%)	81 (99.49%)	73.30
2-CNMBA	6.11×10^{-3}	4267 (46.19%)	6350 (32.73%)	10714 (20.95%)	13782 (13.95%)	35.02
	20.37×10^{-3}	71 (99.10%)	102 (98.92%)	264 (98.05%)	873 (94.55%)	72.76

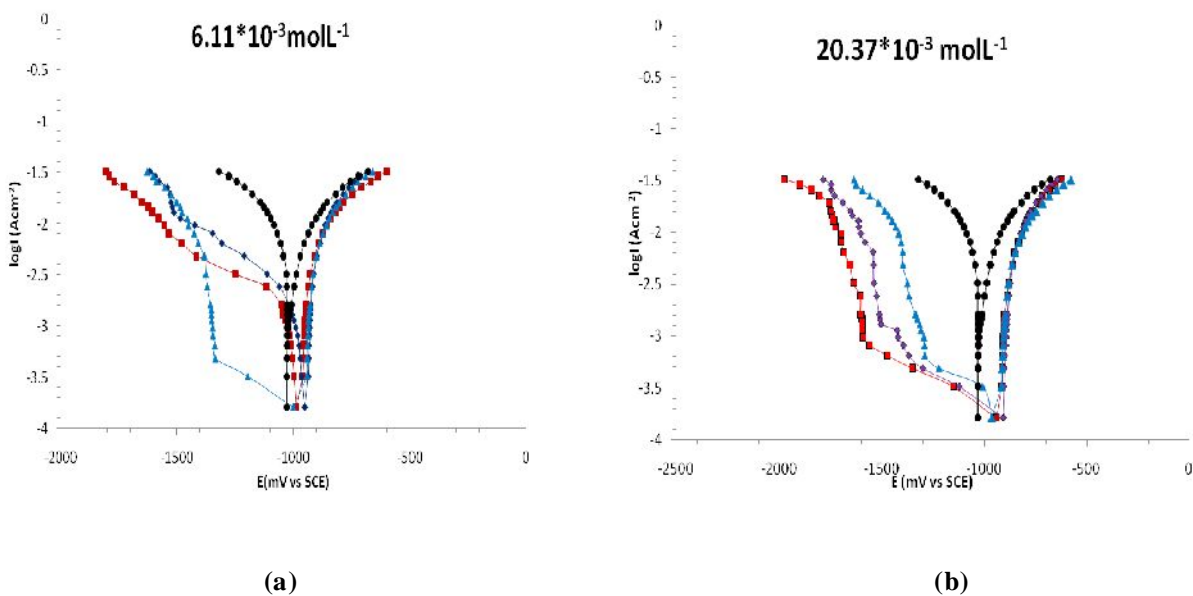


Figure 4: Anodic and cathodic polarization curves obtained for Zinc metal at $35^\circ\text{C} \pm 0.5^\circ\text{C}$ in 0.5M HCl at (a) 6.11×10^{-3} and (b) 20.37×10^{-3} molL⁻¹ concentration of studied Schiff bases. [Blank (?...?); 2-CNMBA (?...?); 3-CNMBA (? ...?); 4-CNMBA († ...†)]

These results indicate that the addition of the inhibitors in the corrosive solution reduces the anodic dissolution of zinc and slows the cathodic evolution of hydrogen [37-39]. This behaviour indicates that these Schiff bases have

effect on both cathodic and anodic reactions of corrosion process but the effects of inhibition is too small on anodic part and suppresses only cathodic process at higher concentration. Therefore, these compounds are classified as mixed type inhibitors with predominance of cathodic inhibition. All the inhibitors shift the potential (E_{corr}) in the positive direction than those measured in blank (0.5 M HCl) because of the formation of zinc oxide and the protective film produced by inhibitors.

Table 4: Electrochemical parameters of corrosion of zinc in the presence of different concentrations of Schiff bases at 35 ± 0.5 °C and corresponding inhibition efficiencies.

Inhibitor	Concentration molL ⁻¹	E_{corr} (mV)	b_a (mV/dec)	b_c (mV/dec)	I_{corr} for cathodic (A cm ⁻²)	(%IE)
Blank	-	-1019	142	169	4.17×10^{-3}	
4-CNMBA	6.11×10^{-3}	-986	235	517	7.08×10^{-4}	83.02
	20.37×10^{-3}	-940	157	170	1.99×10^{-7}	99.99
3-CNMBA	6.11×10^{-3}	-951	154	207	7.59×10^{-4}	81.8
	20.37×10^{-3}	-905	157	170	4.47×10^{-5}	98.93
2-CNMBA	6.11×10^{-3}	-1000	303	400	1.99×10^{-3}	52.17
	20.37×10^{-3}	-961	181	294	1.41×10^{-4}	96.6

The values of cathodic Tafel slope (b_c) and anodic Tafel slope (b_a) calculated from the linear region of the polarization curves, are given in Table 4. The corrosion current density (I_{corr}) was determined from the intersection of the linear parts of the cathodic curves with stationary corrosion potential (E_{corr}) [40, 41].

The percentage inhibition efficiency (%IE) was calculated using the following equation:

$$(\%IE) = \frac{I_{corr}^0 - I_{corr}}{I_{corr}^0} \times 100 \quad (7)$$

where, I_{corr}^0 and I_{corr} are the corrosion current densities in the absence and presence of the inhibitor respectively.

The inhibition efficiencies obtained by extrapolation of the cathodic Tafel line to corrosion potential agree well with those calculated from weight loss data.

3.5 Electrochemical impedance measurements

This technique based on the measurement of the impedance of the double layer at the metal/solution interface. Nyquist plots were obtained for frequency range 30 kHz to 1 Hz at the open circuit potential for zinc in 0.5 M HCl in the presence and absence of inhibitors.

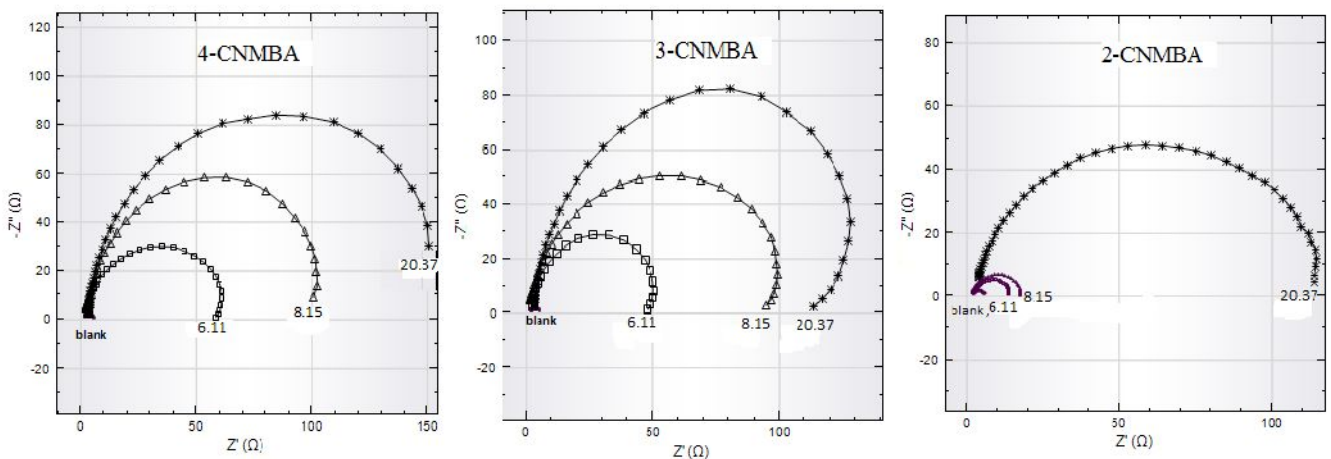


Figure 5: Comparison of corrosion of Zinc exposed in different concentrations ($x \times 10^{-3}$ molL⁻¹) of studied inhibitors by EIS. (a) 4-CNMBA (b) 3-CNMBA (c) 2-CNMBA

The Nyquist diagrams in Figure 5 (a, b and c) show a single semicircle, shifted along the real impedance axis (Z_{real}), indicating that the corrosion of zinc in 0.5 M HCl is controlled by a charge-transfer process [42, 43]. The

impedance spectra for the Nyquist plots were analysed by fitting to the equivalent circuit model as shown in Figure 6. The circuit comprises a solution resistance (R_s), in series with the parallel combination of the charge transfer resistance (R_{ct}) and a constant phase element (CPE).

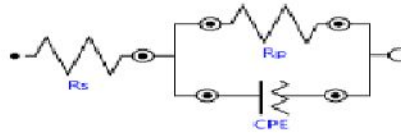


Figure 6: The equivalent circuit model (Randle’s model) used to fit the experimental results of EIS.

The capacitance loops are not exactly semicircle in shape because of the roughness and other inhomogeneity of zinc surface resulting in phenomenon called dispersing effect [44-48]. The charge transfer resistance (R_{ct}) values were obtained from the difference in impedance at lower and higher frequencies [49]. To obtain the double layer capacitance (C_{dl}), following equation was used.

$$C_{dl} = \frac{1}{\omega R_{ct}} \quad (8)$$

Here ω is angular frequency.

$$\omega = 2\pi f_{max} \quad (9)$$

where, f_{max} is the frequency at which the imaginary component of the impedance is maximum ($-Z_{imag}$). The inhibitor efficiency of the inhibitors calculated using:

$$(\%IE) = \frac{R_{ct} - R_{ct}^0}{R_{ct}} \times 100 \quad (10)$$

where, R_{ct}^0 and R_{ct} are charge transfer resistance for zinc in 0.5M HCl in the absence and presence of inhibitors respectively.

Table 5: Electrochemical parameters of corrosion of zinc in the presence of different concentration of Schiff bases at 35 ± 0.5 °C and corresponding inhibition efficiencies obtained from EIS.

Inhibitor	Concentration (molL ⁻¹)	R_s (ohm)	R_{ct} (ohm)	C_{dl} (μF)	(%IE)
Blank	-	0.688	5.99	183	-----
4-CNMBA	6.11×10^{-3}	1.10	63.8	4.22	90.61
	8.15×10^{-3}	3.06	111	2.75	94.60
	20.37×10^{-3}	2.86	149	2.61	95.98
3-CNMBA	6.11×10^{-3}	2.14	52.1	3.27	88.50
	8.15×10^{-3}	0.58	107	3.95	94.40
	20.37×10^{-3}	3.28	137	2.82	95.63
2-CNMBA	6.11×10^{-3}	1.47	13.6	45.40	55.96
	8.15×10^{-3}	1.44	16.4	17.80	63.50
	20.37×10^{-3}	1.97	120	3.69	95.01

In EIS, value of R_{ct} reflects the degree of difficulty in corrosion reaction. As the value of R_{ct} increases, the corrosion rate decreases [50]. It is observed from Table 5 that the values of the charge transfer resistance (R_{ct}) increases with increase in concentrations of inhibitors. This indicates that the charge transfer reactions occurring at the protective film are strongly restricted by the adsorbed inhibitor molecules. The magnitude of double layer

capacitance decreases with increase in inhibitors concentrations. It may be due to decrease in local dielectric constant and/or an increase in the thickness of the electrical double layer and/or a decrease in active area, and therefore suggest that all the inhibitors function by adsorption at the zinc-solution interface [51]. It is worth noting that the change in concentration of inhibitors did not change the profile of the impedance behaviour, suggesting similar mechanism for the corrosion inhibition of zinc by inhibitors.

The %IE obtained by all the three methods agrees well with each other. The small differences between the electrochemically determined corrosion rate and the gravimetrically determined corrosion rate may arise from different reasons, one of them is that the corrosion current is an instantaneous parameter and is a function of time. Depending on the conditions, the corrosion current may decrease or increase with time. On the other hand, the corrosion rates measured by gravimetric methods are time averaged. A unique advantage of the electrochemical techniques is that these can be used to measure the initial corrosion activity of a freshly exposed metal surface, which usually cannot be assessed by using a gravimetric method.

Conclusion

1. Inhibition efficiency increases with increase in inhibitors concentration above a critical concentration and the order is; 2-CNMB < 3-CNMB < 4-CNMB while inhibition efficiency decreases with rise in temperature.
2. Galvanostatic polarisation studies show that studied Schiff bases are mixed type of inhibitors with predominance of cathodic inhibition.
3. From EIS studies, it is observed that R_{ct} value increases and C_{dl} value decreases with increase in concentration of inhibitors which could be resulting from a decrease in local dielectric constant and/or increase in thickness of the inhibitors through adsorption at the metal-solution interface.
4. The adsorption of studied inhibitors is found to follow the Langmuir's adsorption isotherm in acidic media indicating that the inhibition occurs via adsorption. The occurrence of a mixed adsorption (chemisorption as well physisorption) mechanism for the studied inhibitors on zinc surface is supported by the pattern of variation of inhibition efficiency with temperature and values obtained for free energies of adsorption. Further, the adsorption of studied inhibitors on zinc surface is spontaneous and exothermic.
5. Apparent activation energy (E_a) values increase with increase in inhibitors concentration suggesting that inhibition efficiencies increase with increase in inhibitors concentration

Acknowledgements-The authors are grateful to Chemistry Department, School of Sciences, Gujarat University, Gujarat, for the laboratory facilities.

References

1. El-Etre A.Y., Abdallah M., El-Tantawy Z.E., *Corros. Sci.* 47 (2005) 385–395.
2. Abdallah M., El-Etre A.Y., Moustafa M.F., *Port. Electrochim. Acta*, 27 (2009) 615–630.
3. Foad El-Sherbini E.E., Abd El-Wahaab S.M., Deyab M., *Mater. Chem. Phys.* 89 (2005) 183–191.
4. Abdel Fattah A.A., Mabrouk E.M., Abd El-Gulil R.M., Ghoneim M.M., *Bull. Chim. Fr.* 127 (1991) 48–53.
5. Desai M.N., Talati J.D., Shah N.K., *Anti-Corros. Methods and Materials* 55 (2008) 27–37.
6. Abdallah M., *Corros. Sci.* 45 (2003) 2705–2716.
7. Fouda A.S., Elasklany A.H., Madkour L.H., *J. Ind. Chem. Soc.* 61 (1984) 425–429.
8. Fouda A.S., Madkour L.H., *Bull. Chim. Fr.* 5 (1986) 745–749.
9. Fouda A.S., Mohamed A.K., Mostafa H.A., Hussein E.M., *J. Ind. Chem. Soc.* 66 (1989) 417–419.
10. Fouda A.S., Madkour L.H., El-Shafei A.A., Maksoud S.A., *Korean Chem. Soc.* 16 (1995) 454–458.
11. El-Gaber A.S., Fouda A.S., El-Desoky A.M., *Ciencia Tecnologia dos Materiais* 20 (2008) 71–77.
12. Fouda A.S., Abdallah M., Atwa S.T., Salem M.M., *Mod. Appl. Sci.* 4 (2010) 41–55.
13. Shanbogh A.V., Venkatesh T.V., Prabhu R.A., Praveen B.M., *Bull. Mater. Sci.* 34 (2011) 571–576.
14. Eddy N.O., Ebenso E.E., Ibok U.J., Akpan E.E., *Int. J. Electrochem. Sci.* 6 (2011) 4296–4315.
15. Agrawal Y.K., Talati J.D., Shah M.D., Desai M.N., Shah N.K., *Corros. Sci.* 46 (2004) 633–651.
16. Aytac A., Ozmen U., Kabasakaloglu M., *Mater. Chem. Phys.* 89 (2005) 176–181.
17. Li S.L., Chen S., Lei S.B., Ma H., Yu R., Liu D., *Corros. Sci.* 41 (1999) 1273–1287.
18. Yurt A., Ulutas S., Dal H., *Appl. Surf. Sci.* 253 (2006) 919–925.
19. Shah M.D., Patel A.S., Mudalliar G.V., Shah N.K., *Port. Electrochim. Acta* 29 (2011) 101–113.
20. Musa A.Y., Jalgham R.T., Mohamad A.B., *Corros. Sci.* 56 (2012) 176–183.
21. Joseph B., Joseph A., *Port. Electro. Chim. Acta* 29 (2011) 253–271.
22. Milonjic S. K., *J. Serb. Chem. Soc.* 72 (2007) 1363–1367.
23. M.Messali, *J. Mater. Environ. Sci.* 2(2) (2011) 174–185.
24. Aljourani J., Raeissi K., Golozar M.A., *Corros. Sci.* 51 (2009) 1836.

25. Avci G., *Colloids Surfaces A* 317 (2008) 730.
26. Amar H., Tounsi A., Makayssi A., Derja A., Benzakour J., Outzourhit A., *Corros. Sci.* 49 (2007) 2936.
27. Zhang F., Tang Y., Cao Z., Jing W., Wu Z., Chen Y., *Corros.Sci.* 61 (2012) 1-9.
28. Eddy N.O., Idris S.O., Siaka A.A., Magaji L., *New Clues in Sci.* 1 (2011) 102-114.
29. Bahrami M.J., Hosseini S.M.A., Pilvar P., *Corros. Sci.* 52 (2010) 2793-2803.
30. Behpour M., Ghoreishi S.M., Mohammadi N., Soltani N., Salavati-Niasari M., *Corros. Sci.* 52 (2010) 4046.
31. Ahamad I., Prasad R., Quraishi M.A., *Corros. Sci.* 52 (2010) 933-942.
32. Eddy N.O., *Int. J. Phys. Sci.* 4 (2009) 1-7.
33. Sheatty D.S., Shetty P., Nayak H.V.S., *J. Chid. Chem. Soc.* 51 (2006) 849-853.
34. Eddy N.O., Ebenso E.E., Ibok U.J., *J. Argent. Chem. Soc.* 97 (2009) 178-194.
35. Okafor P.C., Ebenso E.E., *Pigment & Resin Technology* 36 (2007) 134 – 140.
36. Eddy N.O. *Port. Electrochim. Acta* 27 (2009) 579-589.
37. Finšgar M., Lesae A., Kokalj A., Milošev I., *Electrochim. Acta* 53 (2008) 8287-8297.
38. Lebrini M., Lagrenee M., Traisnel M., Gengembre L., Vezin H., Bentiss F., *Appl. Surf. Sci.* 253 (2007) 9267.
39. Salah S. Al-Luaibi, Seta Azad, Abdul Amir H.Taobi, *J.Mater. Environ. Sci.* 2 (2) (2011) 148-155.
40. Mistry B.M., Patel N.S., Sahoo S., Jauhari S., *Bull. Mater. Sci.* 35 (2012) 459-469.
41. Abd EI-Maksoud S.A., Fouda A.S., *Mater. Chem. Phys.* 93 (2005) 84-90.
42. Goulart C.M., Souza A.E., Huitle C.A.M., Rodrigues C.J.F., Maciel M.A.M., Echevarria A., *Corros. Sci.* 67 (2013) 281.
43. Aisha M. Al-Turkustani, Sanaa T. Arab, Reema H. Al-Dahiri, *J.Mater. Environ. Sci.* 3 (6) (2012) 1163.
44. Ramesh S., Rajeswari S., *Electrochim. Acta* 49 (2004) 811.
45. Bostan R., Varvara S., Gaina L., Muresan L.M., *Corros. Sci.* 63 (2012) 275-286.
46. Tang Y.M., Yang W.Z., Yin X.S., Liu Y., Wan R., Wang J.T., *Mater. Chem. Phys.* 116 (2009) 479-483.
47. Behpour M., Ghoreishi S.M., Salavati-Niasari M., Ebrahimi E., *Mater. Chem. Phys.* 107 (2008) 153-157.
48. N.A. Al-Mobark, K.F. Khaled, O.A. Elhabib, K.M. Abdel-Azim, *J.Mater. Environ. Sci.* 1 (1) (2010) 9-19.
49. John S., Mohammad K., Joseph A., *Bull. Mater. Sci.* 34 (2011) 1245-1256.
50. Feng L., Yang H., Wang F., *Electrochim. Acta* 58 (2011) 427-436.
51. Bentiss F., Mernari B., Traisnel M., Vezin H., Lagrenee M., *Corros. Sci.* 53 (2011) 487-495.

(2014) ; <http://www.jmaterenvironsci.com>